Letters 8, 87 (1962).
[11]C. W. Higginbotham, F. H. Pollak, and M. Cardona, in *Proceedings of the Ninth International Conference on Physics of Semiconductors* (Nauka, Leningrad, 1968), Vol. I, p.57.

PHYSICAL REVIEW B VOLUME 3, NUMBER 10 15 MAY 1971

Brillouin-Scattering Analysis of Phonon Interactions in Acoustoelectric Domains in GaAs†

E. D. Palik* and Ralph Bray
Physics Department, Purdue University, Lafayette, Indiana 47907
(Received 29 June 1970)

Acoustoelectrically amplified domains of ultrasonic flux in GaAs were used for analyses of various phonon interactions by Brillouin-scattering techniques. Both the growth of the flux from the thermal equilibrium phonon spectrum and particularly the attenuation (after the amplifying voltage pulse was shut off) were studied as a function of ultrasonic frequency in the broad range from 0.3 to 4.0 GHz at 300 °K. The data were analyzed to give the magnitude and frequency dependence of both the acoustoelectric gain and the lattice attenuation in the weak-flux regime. Comparison with small-signal gain theory in the $ql \approx 1$ range, for piezoelectrially active [110] shear waves, gave good agreement. The lattice attenuation was determined not only for the amplified shear waves but also for the piezoelectrically inactive longitudinal waves, which were obtained by mode conversion upon reflection of the amplified shear-wave domain. The frequency dependence of the attenuation, proportional to $f^{1.8}$ and $f^{1.3}$, respectively, fell well below the expected f^2 behavior. In the strong-flux regime, striking anomalous attention was found, consisting of a too-rapid initial attenuation of low frequencies, and too-slow initial attenuation of higher frequencies. These results are interpreted to represent a dominant trend of up-conversion of intense ultrasonic flux from low to high frequencies by nonlinear frequency-mixing processes. Evidence is summarized favoring such frequency-mixing processes, over possible variation in the frequency dependence of the acoustoelectric gain in strong flux, as a dominant factor in the evolution of the strong-flux spectrum both in growth and attenuation.

I. INTRODUCTION

Domains of intense acoustic flux, containing a rather broad band of frequencies in the low-GHz range, can be produced in piezoelectric semiconductors by acoustoelectric amplification of phonons from the thermal equilibrium spectrum.[1,2] By means of Brillouin-scattering techniques,[2] it is possible to use such domains to follow the growth and attenuation of the various frequency components of the amplified acoustic flux and thus study various types of phonon interactions as a function of phonon frequency and intensity. Those studied in some detail in the present work include (a) the acoustoelectric interaction,[3] a term applied here in the restricted sense of referring only to the exchange of energy and momentum between the electrons and the beam of amplified phonons, (b) the ordinary lattice attenuation of the amplified flux via the nonelectronic interaction with the thermal phonons of the lattice, and (c) phonon-phonon interactions of electronic origin which are a nonlinear extension[4-6] of the acoustoelectric interaction and arise from the interaction of bunched electrons of one frequency with the piezoelectric fields associated with other frequencies. The resulting nonlinear mixing of frequencies and parametric interactions cause up- and down-conversion in the frequencies of the acoustoelectrically amplified flux.

In analyzing these phonon interactions, we are faced with two problems: In general, the interactions coexist, making it necessary to devise methods of distinguishing them from one another; and the interactions are, in different degree, dependent on the intensity and spectral composition of the amplified flux. In sufficiently weak flux, where only the small-signal acoustoelectric and lattice-attenuation processes are present, these interactions can be separated fairly easily by making growth or attenuation measurements under variable current conditions, since only the acoustoelectric interaction is current dependent. The analysis becomes much more difficult in strong flux where deviations of the growth and attenuation from small-signal theory become evident. A most important observation there is the rapid shift and continued evolution of the spectral distribution of the amplified acoustic flux as it continues to grow.[2,7] The problem of interpretation boils down to distinguishing between (i) a shift in the frequency dependence of the acoustoelectric interaction in strong flux and (ii) the onset of mixing and frequency conversion of the acoustic flux via interaction (c) above.

Our investigation of these problems was restricted

to semiconducting n-GaAs at room temperature, where the amplified acoustic flux available and accessible for study was in the band 0.3–4.0 GHz. The work is an extension of that of Spears[2] on the same material. Whereas Spears was concerned mainly with following the acoustic flux during amplification, we have extended the study to the attenuation regime after the amplifying voltage pulse is cut off.[8] This has provided a much richer picture of the various phonon interactions. In order to discuss the specific objectives and new results of the present investigation, we shall first summarize the previous work. A fairly complete statement is necessitated by the existence in the literature of controversies and conflicting interpretations of important aspects of the phenomena occurring within the acoustoelectric domain.

The flux in the domain consists of piezoelectrically active[9] fast shear waves, propagating along the length of the sample in the [110] direction. The domain, a few mm wide in GaAs, propagates with the velocity of these waves, 3.35×10^5 cm/sec. The formation of propagating domains[1,2] is a consequence of several factors, including (a) the fact that the acoustic flux itself is propagating, (b) the inevitable inhomogeneities[10] in the resistivity of the sample and hence in the acoustoelectric gain, which permits nonuniform growth of flux in the sample, and (c) feedback effects consisting of redistribution of voltage in the sample produced by the nonuniform buildup of the acoustic flux and the resulting drop in current. The early stages of domain formation have been quantitatively explained in just these terms within the framework of the small-signal acoustoelectric theory. Later stages in the evolution of domains involve changes in the spatial and frequency distribution of the acoustic flux,[11] and the problem there really becomes one of determining and understanding the dominant interactions occurring in the strong-flux regime.

The composition of phonons in the domain is determined by the fact that the amplification process is selective both in frequency and propagation direction. In GaAs, the acoustoelectric interaction is strongest for the piezoelectrically active fast shear waves propagating in the [110] direction. Because of the angular dependence of the gain, the amplified acoustic flux quickly assumes a beam-like character, becoming contained in a narrow wave-vector cone of about 10° half-width around the [110] direction.[2] We shall be interested here only in the on-axis flux. In this case, the acoustoelectric energy gain in relatively high-conductivity material[1,9] is given by $\alpha_0\gamma$, where $\gamma=v_d/v_s-1$; v_d is the electron drift velocity and v_s is the velocity of the fast shear waves. The frequency dependence[12] of the amplified flux is contained in the material-dependent coefficient α_0, which depends on the parameter ql, the product of phonon wave vector and electron mean free path. The frequency of maximum gain is given by $f_m=(\omega_\sigma\omega_D)^{1/2}/2\pi$ for $ql\ll1$ and $(3\omega_\sigma\omega_D)^{1/2}/2\pi$ for $ql\gg1$, where $\omega_\sigma=\sigma/\epsilon$ is the dielectric relaxation frequency and $\omega_D=v_s^2/D$ is the diffusion frequency with $D=\mu kT/e$. Here σ is the dc conductivity, ϵ is the dielectric constant, and μ is the electron mobility. In the present material, $ql\approx1$ and a numerical evaluation[13] of α_0 is required which gives an f_m intermediate between the two extremes. The net gain is given by $\alpha_n=\alpha_0\gamma-\alpha_l$, where $-\alpha_l$ represents the lattice attenuation. Because of the frequency dependence of the latter, the frequency of maximum *net* gain is shifted slightly below f_m, close to 3 GHz in our material.

The weak-flux regime is operationally defined by the range of validity of the approximation that α_0 and α_l are flux independent, and that γ continues to be given by v_d/v_s-1, with v_d in the domain given by J/ne, where J is the current density and n the free-electron concentration. In this case, flux of energy density ϕ propagates with velocity v_s along the sample in the direction of current and, while propagating, grows at a rate given[1,2] by

$$\frac{d\phi}{dt}=\alpha_n\phi+c\phi_0\,, \tag{1}$$

where $c=\alpha_0+\alpha_l$. The term $c\phi_0$ permits $d\phi/dt$ to be equal to zero when $v_d=0$ and $\phi=\phi_0$, the thermal equilibrium value of flux propagating in the direction of the anode. Thus, after a time t, the flux ϕ_0 starting at any position x has propagated a distance v_st, and for constant current and gain has grown to

$$\phi\cong\phi_0(1+c/\alpha_n)e^{\alpha_nt} \tag{2}$$

for $\phi\gg\phi_0$. Exponential growth becomes the empirical criterion for the weak-flux regime. To observe this condition, it is critically important to make measurements sufficiently early in the growth. The most definitive study of the range of applicability of the weak-flux regime was made by Spears[2] in GaAs at 300 °K. The flux growth at the frequency of maximum net gain $f_m\approx3$ GHz was found to be exponential and in good accord with small-signal theory up to intensities of about 10^8 greater than the calculated thermal equilibrium value. The frequency of maximum net gain and the bandwidth of the amplified flux all checked well with theory, as did the angular distribution of the flux and its spatial distribution in domains. Other experimental studies,[14–16] in CdS at 300 °K where $ql\ll1$, were restricted to showing only that the early flux growth does peak close to the expected value of f_m.

The termination of the weak-flux regime in n-GaAs is signified by the tendency of the flux at f_m to saturate.[2] This occurs when the flux growth

at f_m exceeds the factor 10^8, and the total amplified energy density approaches about 10^{-2} J/cm^3. At the same time, a rapid upsurge[2,17] is noted in the growth rate at lower frequencies, the growth being much too rapid to be accounted for by small-signal gain theory. Thereafter, there is a progressive evolution of the frequency spectrum in which ever lower frequencies begin to build up rapidly. Ultimately, the peak intensity of the flux can shift down to frequencies of about $\frac{1}{10} f_m$. The downshift in the frequency spectrum was first observed by Zucker and co-workers[7,18] in CdS, where it was verified by several investigators.[14-16] Since it occurs both in CdS and GaAs, it appears to be a characteristic feature of strong flux in piezoelectric semiconductors.

The observation of this evolution of the frequency spectrum has generated much theoretical interest and more detailed experimental work. Most of the theories have been directed to showing that the acoustoelectric gain is modified in strong flux in such a way as to lower the frequency of maximum gain.[14,19-22] These theories have generally failed to take into consideration the evidence accumulating from the experimental side for parametric amplification[7] of subharmonics of f_m, attributed to the phonon-phonon interactions of electronic origin. The evidence consists of the following observations: (a) Zemon *et al.*,[23] using strong microwave-injected flux at f in CdS, observed its conversion first to $\frac{1}{2}f$ and then to $\frac{1}{4}f$, thus demonstrating the possibility of this interaction. (b) Its importance in the amplified acoustic domain was demonstrated first[17] in GaAs and then[24] in CdS by the observations that the transition from the small-signal regime is not smooth but rather discontinuous; i.e., the initial growth spurt at $f < f_m$ was greatest near $\frac{1}{2}f_m$, where a subsidiary peak in intensity was formed which rapidly exceeded the original peak at f_m. This transition in GaAs was seen[11] to occur spatially only in the intense core of the domain, attesting to the flux dependence of the process. (c) Microwave emission[25] and current noise[26] studies from amplified domains revealed the formation of peaks at subharmonics of f_m, both in GaAs and in CdS. Thus it appears that the acoustoelectrically amplified flux near f_m acts as a pump to amplify the subharmonic frequencies, at least in the first stage of the down-conversion of the frequency spectrum.

No comparable direct evidence of the modification of the acoustoelectric gain producing downshift of f_m in strong flux can be cited. Nevertheless, there is no reason to believe that such an effect may not contribute to the complex downshift pattern of the acoustic spectrum. The problem remains to further discriminate experimentally between the roles of frequency conversion and modification of the direct acoustoelectric gain, and to provide an integrated theoretical picture of the different processes.

We may turn now to the several objectives of the present study. The first was simply to develop methods to use the domain as a broad-band source of acoustic flux to measure the small-signal acoustoelectric gain and lattice-attenuation parameters over the widest possible frequency range. Data for these parameters had been obtained by Spears[2] for flux at 3.1 GHz during the growth process. However, there are definite limitations to making such measurements during the initial amplification process, since the growth of flux of measurable intensity is restricted to frequencies near f_m. In the present material and with our present sensitivity, this constitutes the band 2–4 GHz. In the present work this frequency range was extended by permitting the acoustic flux to build up to the strong-flux regime where intense flux at lower frequencies was produced. The amplifying voltage pulse was then cut off and the flux permitted to attenuate back to the small-signal regime, leaving copious amounts of the slowly attenuating low-frequency components in the range 0.3–2.0 GHz. This flux was used either for attenuation or growth studies, depending on externally imposed bias conditions. Thus, by the combination of growth and attenuation studies, the broad frequency range 0.3–4.0 GHz was investigated. The net acoustoelectric gain was measured and the separation of the acoustoelectric and lattice-attenuation parameters effected by making such measurements as a function of bias current. A by-product of the present investigation was the measurement of the attenuation of piezoelectrically inactive [110] longitudinal waves. This flux was obtained by mode conversion from the amplified shear waves, upon reflection of the latter at the downstream end of the sample. The two modes can be readily distinguished by their different velocities and by the different polarization conditions for Brillouin scattering. The data obtained in this way for both modes greatly exceed in scope those available from conventional measurements at room temperature. The methods described here for generating a broad band of high-frequency flux and measuring rapid growth or attenuation should be applicable to other materials.

The second objective of the present study was to investigate further the strong-flux regime. In the course of following the attenuation of the acoustic flux, we found interesting new aspects of the interactions in strong flux. In particular, an apparent strong conversion of flux from low to high frequencies was observed during attenuation, just the reverse of the previous observations during flux growth.[2] This evidence for the greater scope of the mixing and frequency-conversion processes

strengthens the argument for their importance in determining the evolution of the spectrum of the acoustic flux. The question is discussed of the significance of the transition from dominant down-conversion of frequencies during flux growth to up-conversion during flux attenuation.

II. EXPERIMENTAL CONDITIONS AND ANALYSIS OF BRILLOUIN SCATTERING

With the use of Brillouin-scattering techniques, it is possible to follow the changes in spectral composition of the amplified-phonon spectrum in space or time, but not without some inherent limitations on the resolution, on the range of frequencies that can be covered, and on the interpretation of the phonon intensity. A comprehensive discussion of the method and its limitations in GaAs has been given by Spears.[2] We give here only the essential features needed for the present study.

The Brillouin-scattering geometry is illustrated in Fig. 1. Light of wave vector $\vec{k}_0$ is shown scattered through the internal angle θ', within the sample by absorption of a phonon of wave vector $\vec{q}$, to produce the scattered-light wave vector $\vec{k}_s$, where $\vec{k}_s \approx \vec{k}_0$. Then $\vec{q} = 2\vec{k}_0 \sin\frac{1}{2}\theta'$. Our interest here is restricted to phonons propagating along the axis of the sample. In this case we need only measure the external scattering angle θ, which is set equal to twice the incident angle ψ, in order to obtain the phonon frequency given by

$$f = (2v_s/\lambda_0)\sin\tfrac{1}{2}\theta \ . \qquad (3)$$

Here λ_0 is the optical wavelength in vacuum. With the sound velocity known, only light-scattering angles, and not frequency shifts, need be directly measured. Hence the Brillouin-scattering apparatus can be quite simple. The phonon velocity v_s is equal to 3.35×10^5 cm/sec for fast shear waves propagating along the [110] axis, as can be verified from careful measurements of the domain velocity.[10] Either the Stokes (phonon emission) or the anti-Stokes (phonon absorption, as shown) scattering can be measured with equivalent results.

A. Experimental Arrangement

The optical setup contains a high-pressure Hg lamp, pulsed to give additional intensity, much above the dc operating level. The light was collimated, filtered, polarized by an Ahrens prism, and focused on the sample. The slit image was usually set between 0.5 and 1 mm. This gave fair spatial resolution of the propagating domain whose width and shape are somewhat variable with frequency and time; however, the width is always greater than 1 mm in GaAs. The sample was placed on a rotatable mount which served to determine the angle of incidence ψ of the light. The system for detecting the scattered light was attached to a rotating arm which was used to select the desired scattering angle. The scattered light was analyzed by another Ahrens prism to select light with polarization rotated by 0° or 90° in the scattering process. It was then passed through a small square aperture to define a portion of the scattered light cone and focused on a Si diode detector. The effective spectral bandwidth of the light source was limited to $\lambda_0 > 0.9\ \mu$ by the absorption edge of GaAs and $\lambda_0 < 1.1\ \mu$ by the Si photodetector response; this could be further restricted by narrow-band filters when necessary.

The GaAs sample used in these experiments had dimensions $2.2\times0.17\times0.065$ cm^3. It was cut with the [110] axis along the long dimension and the [001] axis along the intermediate dimension. The two large faces were optically polished by conventional methods. Leads were attached with indium solder to both ends to make Ohmic contacts. The sample resistivity at room temperature was 1.27 Ω cm.

Synchronization of optical and electric pulses were necessary to measure scattering from the propagating domain when the pulsed light source was at its peak intensity. The domain was generated by the application to the GaAs sample of a pulse of about 2500 V and several μsec duration. This was triggered through a variable delay from the pulse which fired the Hg lamp. The domain was timed to reach the focused light spot just when the latter was at the peak intensity. A second voltage pulse, usually less than 300 V, was applied to the sample just after the primary pulse was terminated This supplied a variable bias to be used for controlling the acoustoelectric contribution to the attenuation of the domain. The transient response of the detector to the scattered-light pulse, produced by the passage of a domain, was amplified by a Tektronix 1A1 plug-in preamp, displayed on an oscilloscope, and photographed.

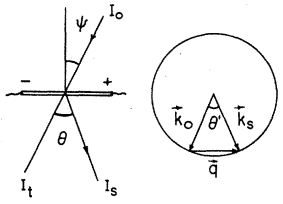

FIG. 1. Sample geometry for observing Brillouin scattering. The external scattering angle θ is shown at the left while the internal scattering angle θ' is shown at the right.

B. Limitations on Frequency Range and Resolution

The frequency range over which acoustic flux can be detected is about 0.3–6.0 GHz, thus encompassing the frequency of maximum gain of ~3.0 GHz, and the down-conversion of flux by a factor of 10. The high index of refraction of 3.5 in GaAs and resultant internal reflection of light limits θ'

to 16.7° and sets an upper limit of 6.7 GHz for detecting acoustic frequencies when $\lambda_0 \approx 1\ \mu$.

A lower limit of 0.3 GHz is set for analyzing the low-frequency flux which scatters light through very small angles. The angular resolution depends on the minimum size of the aperture of the detector and its optics with which scattered signals could be measured. The aperture determines the fraction of the scattered-light cone which is accepted by the detector; this, together with the spectral bandwidth of the incident light, determines our resolution of the phonon spectrum. The aperture is the more important factor at low frequencies. A square aperture giving a 4.5° cone was usually used for phonon frequencies above 1 GHz, while below this it was necessary to reduce the cone to 2° or 3° to maintain resolution. The radiation bandwidth of the light, about 20% centered near 1 μ, contributed an equivalent 20% bandwidth to the determination of the acoustic frequency. Narrow-band filters were inserted to improve the resolution when necessary, but most of the experiments were made with the full bandwidth. The individual contributions to the resolution by the two factors are indicated in Fig. 8.

C. Polarization Conditions and Mode Identification

The shear and longitudinal waves studied in this work are identified both by their velocities and the polarization selection rules[2,27] for scattering. For either case, we can take light incident on the $(1\bar{1}0)$ surface, with polarization either along the [001] or [110] direction. For fast shear waves (TA) propagating in the [110] direction and polarized along the [001] direction, the light is scattered strongly with a 90° rotation of polarization. Longitudinal waves propagating along the same [110] direction scatter light without rotation of polarization. Thus the orientation of the polarizer with respect to the analyzer can be used to discriminate in favor of one or the other mode. Since the LA mode is not amplified but produced only as a by-product of the TA mode by mode conversion upon reflection at the anode, it gives very small scattering signals.

The above discussion is illustrated in the photographs in Fig. 2 of incident and reflected domains for the two polarization selection rules. Each trace represents the time variation of the Brillouin-scattering signal from a domain as it passes the light spot. The various traces are obtained at the indicated successive positions of the light probe along the sample. The propagation of domains in the forward direction, i.e., from cathode to anode, is evident and the domain velocity is easily determined. Near the anode, where the reflection takes place, the incident and reflected signals occur closer in time. Note that near the cathode, the signal of the returning domain after reflection from the anode can be larger than the original forward-traveling signal. This happens primarily for low-frequency flux which is not built up till the forward-traveling domain becomes intense; but after reflection, it attenuates very slowly and may be observable all the way back to the cathode and even once again after reflection there. In Fig. 2(a) the polarization condition is given by $A \perp P \parallel [001]$, where A represents the analyzer and P the polarizer. This is the condition for detecting only the fast TA waves. For the experimental condition $\theta = 7°$, $\psi = 4°$, we show flux of $f = 0.41$ GHz, traveling ~1° off axis. There is no evidence here of contribution from a LA mode. In Fig. 2(b) the polarization condition is $A \parallel P \parallel [001]$, which is favorable for detecting only the LA waves. The LA waves, which are faster than the TA waves, show up only in reflection, as indicated on the figure. Their frequency here is 0.64 GHz. However, we still see weak signals from the incident and reflected fast TA waves. These are much weaker than in the upper half of the figure (as can be seen from the relative signal-to-noise ratios). That there is any signal at all from the TA waves is attributable to an appreciable double scattering of the light by the intense TA flux in the domain.

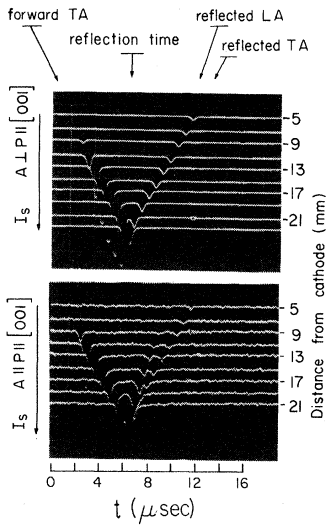

FIG. 2. Top oscilloscope traces in (a) show scattering signals for the forward-propagating and reflected TA phonon domain for the crossed polarizer and analyzer combination required to observe single scattering. Bottom oscilloscope traces in (b) show the forward-propagating TA domain and both the reflected TA and LA domains. Here, a parallel polarizer and analyzer combination is used as required to see the LA domain. Nevertheless, the weak TA domain signals appear in (b) by virtue of double Brillouin scattering in the intense phonon flux, which permits the violation of the crossed-polarization requirement discussed in the text. For $\theta = 7°$ and $\psi = 4°$ we see here 0.41-GHz TA phonons in the single-scattering case and 0.64-GHz LA phonons traveling ~1° off axis.

Two successive 90° rotations of polarization permit the apparent violation of the polarization condition. Because of this multiple-scattering condition, the frequencies of the TA domain cannot be identified now. The identification of the LA phonons was confirmed by determining the velocity to be 5.23×10^5 cm/sec, in agreement with expectations. We could not detect any converted slow TA waves which would travel with a velocity of 2.47×10^5 cm/sec.

D. Determination of Growth and Decay of a Domain

The record of the growth and the decay of a domain as it traverses the sample is shown in Fig. 3. The photograph consists of a multiple exposure of the domain-induced scattering traces $I_s(t)$ at a series of closely spaced positions along the sample. The superimposed traces shown in Fig. 3 represent the shear waves at $f=1.04$ GHz. The corresponding current and voltage pulses are also shown in the figure. The drop in current coincides with the strong growth in the domain signal. After the voltage pulse is cut off, the domain signal attenuates rather slowly, with appreciable amplitude persisting all the way to the end of the sample.

To measure attenuation or gain, it is necessary to "tag" some portion of the domain and follow it as a function of time. For a single domain propagating through the sample, a suitable tag point is the maximum flux in the sample at a *given time*. This is given at each time by a point on the envelope of the superimposed signals. The envelope then represents the time variation of the point of maximum acoustic intensity in the propagating domain. An alternative procedure would have been to determine the spatial distribution of I_s in the sample at each time, which is much more tedious. It should be noted that for a rapidly evolving domain signal, the maximum in a signal $I_s(t)$ observed at a given position (i.e., within a given trace) is not necessarily the same as the maximum flux in the sample at a given time. A failure to appreciate this distinction can cause serious error in the determination of the velocity of the domain.

For sufficiently weak Brillouin scattering, the envelope of I_s represents the time variation in phonon intensity of the chosen frequency component. In the weak-scattering condition, there is negligible depletion of the transmitted (i.e., unscattered) light signal I_t (Fig. 1). When such depletion does occur, it is due to all the possible Brillouin scattering from the amplified cone of acoustic flux. It includes not only the scattering from the on-axis flux of interest here, but also the scattering from the amplified off-axis flux components at other frequencies satisfying the scattering condition. The integrated effect may be very great and give as much as 80% depletion of I_t. Appreciable depletion of I_t has two implications: (a) that I_s is indirectly diminished because of the decrease in the intensity of incident light available for contributing to I_s, and (b) that the signal I_s may be *directly* decreased by secondary scattering before it can pass through the sample. Such effects will obviously distort the dependence of I_s on frequency and on time. A treatment which substantially corrects for this strong scattering was given by Spears[2] under the reasonable approximation that the incident light beam I_0 and the scattered beam of interest are both subject to the same scattering probabilities. Then a simple calculation shows that the normalized ratio I_s/I_t is proportional to the phonon intensity of interest. The ratio should be determined at each point in time along the envelopes of I_s and I_t. The proportionality of I_s/I_t to phonon intensity is frequency dependent,[2] but this does not concern us now.

One of the assumptions involved in the derivation of the above relationship is that the multiple-scattered light is lost, i.e., that it does not end up contributing back to either I_s or I_t. This assumption may break down for very intense flux. However, this difficulty will not arise for the quantitative

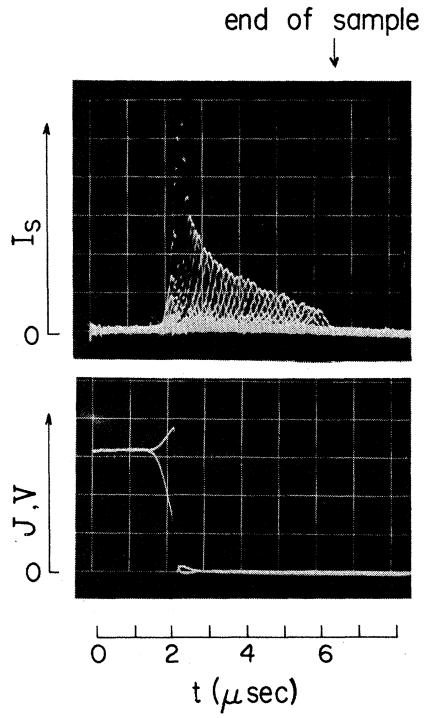

FIG. 3. Envelope of scattering signals I_s as a function of time for the light spot moved progressively down the sample; $\theta=18°$, $f=1.04$ GHz, and $A\perp P\parallel[001]$. From the accompanying current and voltage pulses, we see that the domain signal switches from growth to attenuation when the voltage is cut off.

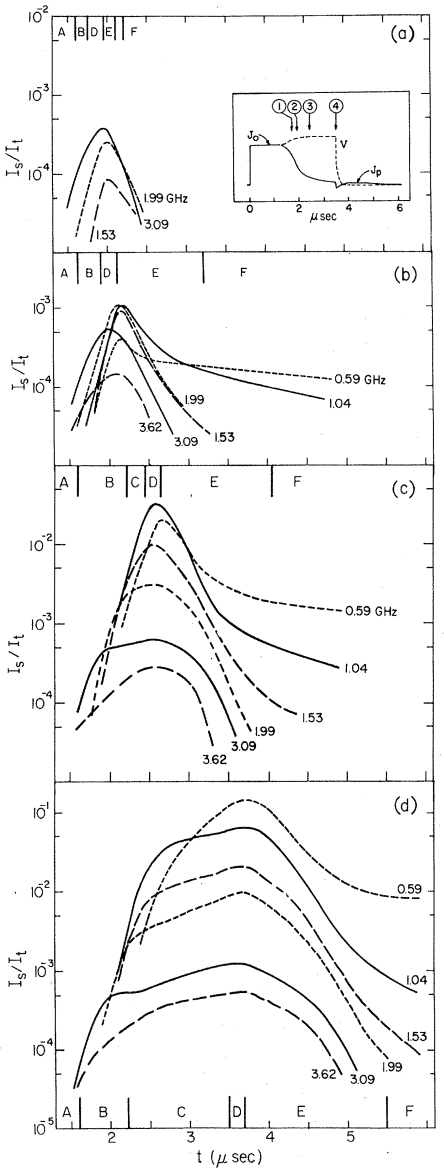

FIG. 4. The scattering ratio I_s/I_t, during growth and attenuation of flux, is shown as a function of time for several indicated frequencies. Distinct regions in growth and attenuation (see text) are labeled A–F. The various voltage cutoff times for (a)–(d) are shown in the inset.

part of our analysis in the weak-flux regime. It can affect the qualitative findings in the strong-flux regime, particularly for the more weakly scattering high acoustic frequencies. A discussion and correction for this effect is given in the Appendix.

III. OVER-ALL VIEW OF EVOLUTION OF PHONON SPECTRUM DURING GROWTH AND ATTENUATION

Photographs of the type shown in Fig. 3 provided the raw data for calculating I_s/I_t (representing the phonon intensity in arbitrary units) and determining the evolution of the phonon spectrum through the various stages of flux growth and attenuation. A comprehensive picture of our results is presented in Fig. 4, which provides the basis for much of our analysis. Sets of growth and attenuation curves of I_s/I_T at the various indicated acoustic frequencies ranging from 0.59 to 3.6 GHz are shown for four successively longer pulses of applied voltage. These provide four sets of data, 4(a)–4(d), of progressively longer intervals of growth of the phonon flux. The data are redundant during the growth stage, but serve the function of providing different initial conditions at the onset of attenuation. This is very important for studying the dependence of the attenuation on the intensity and spectral distribution of the flux. The time at which the voltage pulses were cut off, along with the conditions of current and voltage, are shown in the inset in Fig. 4(a).

The time scale is subdivided into intervals labeled A–F to help identify the various stages of the phonon interactions as the intensity grows and then decays. Thus, A is the interval of early flux growth in which small-signal theory is applicable. Here the growth is centered around $f_m \approx 3$ GHz, as is best seen in Fig. 4(a). The down-conversion to lower frequencies, alluded to in Sec. I, enters in interval B with the appearance of the low frequencies which grow rapidly while the intensity at f_m tends to level off. In C ever lower-frequency components grow rapidly and progressively surpass their predecessors, which level off in turn. In the longest pulses, as shown in Fig. 4(d), we see that there is a tendency for the leveling off in growth of all but the lowest frequencies. The signal is now greatest at 0.59 GHz and still growing rapidly. After 3.5 μsec of applied voltage, a steady-state spectrum is not yet established.

In interval D, the voltage pulse is cut off in about 0.2 μsec. Intervals E and F correspond to the attenuation stages of the acoustic flux, which are of major interest in the present work. The decay patterns of E are representative of the strong-flux regime, and those in F of the weak-flux regime. In the latter, lattice attenuation is dominant and the low frequencies attenuate very slowly and the higher frequencies more rapidly, as expected. From such data, the separate parameters for the small-signal acoustoelectric and lattice attenuation can be determined mainly for $f < 2.0$ GHz, to complement the data obtainable from growth studies in interval A for $f > 2.0$ GHz. The decay pattern is most interesting in strong flux in interval E. There the low frequencies near 0.59 GHz attenuate anomalously rapidly[8] before achieving their expected slow decay in F. By contrast, the higher frequencies near 3 GHz attenuate anomalously slowly in E before achieving their expected fast decay in F. The comparison of the anomalous decay patterns

in Figs. 4(a)–4(d) provide useful information about the dependence of these strong-flux effects on the initial flux conditions at the beginning of the attenuation stage. The results in the weak- and strong-flux regimes will be discussed in detail in Secs. IV and V, respectively.

IV. ANALYSIS IN THE WEAK-FLUX REGIME: ACOUSTOELECTRIC AND LATTICE-ATTENUATION PARAMETERS

The weak-flux regime was studied both during growth in region A and during attenuation in region F of Fig. 4. The results in these two regions are complementary, supplying the high and low ends of the frequency spectrum, respectively. The net gain (or attenuation) α_n was determined at selected values of γ. From the dependence of α_n on γ, the acoustoelectric and lattice-attenuation parameters α_0 and α_l were obtained. Before discussing the results, we have to describe more explicitly how α_n and γ were determined.

A. Determination of α_n under Bias Conditions

It is imperative in regions A or F to ascertain that growth or attenuation is indeed taking place in the small-signal regime where I_s/I_t varies as $e^{\alpha_n t}$. To illustrate the latter, typical semilog plots of I_s/I_t vs time are shown in Fig. 5 for various conditions.

Measurements in the early stages of growth are shown in Fig. 5(b) for several frequencies near f_m, between 2 and 4 GHz, at $\gamma = 22.5$. The growth curves are arbitrarily displaced along the time scale for clarity. The slopes of the straight-line portions yield α_n. The deviations from the drawn lines are presumed to be indicative of departures from the weak-flux regime.

The measurements during the late stages of attenuation (in region F) are made either while the domain is propagating downstream in the last half of the sample, or while the reflected domain is propagating back towards the cathode. The reflection efficiency was about 80% at 0.3 GHz, decreased to 30% at 0.8 GHz, and continued to diminish rapidly with increasing frequency. A subsidiary voltage pulse was applied shortly after the amplifying pulse was cut off, to supply a bias of current density J_b. The latter establishes a value of $v_d = J_b/ne$ and $\gamma = J_b/nev_s - 1$. It is important to note that a fixed value of J_b is not established instantly when the bias voltage is applied, but only after the intense flux has decayed to the level at which it no longer influences the current. This is illustrated in Fig. 6, which will be discussed in more detail below. Suffice it to say that it is necessary to wait till the bias current reaches a steady-state value if attenuation is to be measured at a fixed value of γ. Under such conditions, only the more slowly attenuating lower frequencies can be easily followed.

Representative attenuation data are illustrated in Fig. 5(a) for the case $J_b = 0$ or $\gamma = -1$ for three different frequencies. The straight-line portions on the semilog plot determine the coefficient $\alpha_n = -\alpha_0 + \alpha_l$. In Fig. 5(c) data are shown for a single frequency ($f = 1.04$ GHz) for a range of bias currents corresponding to values of γ between -1 and 5.5. The dependence of the coefficient α_n on the acous-

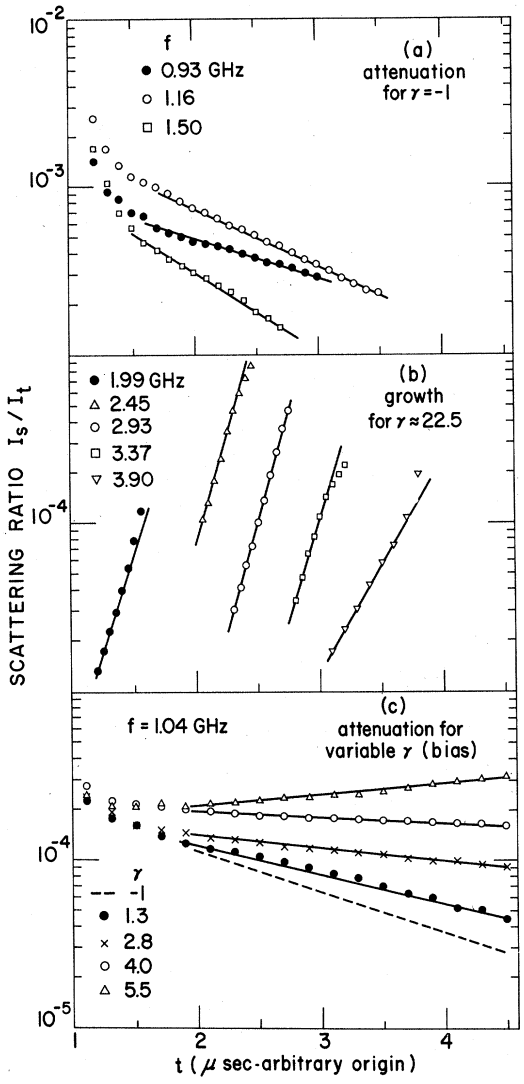

FIG. 5. (a) Scattering ratio I_s/I_t for three frequencies showing their range of exponential attenuation (solid straight lines) in the small-signal regime. (b) I_s/I_t for five frequencies showing their exponential growth near the frequency of maximum gain. The origin of the time scale is arbitrary for each frequency. (c) I_s/I_t for $f = 1.04$ GHz showing its exponential attenuation and growth for several bias currents. No experimental data were obtained for this particular run for $\gamma = -1$ (no external bias).

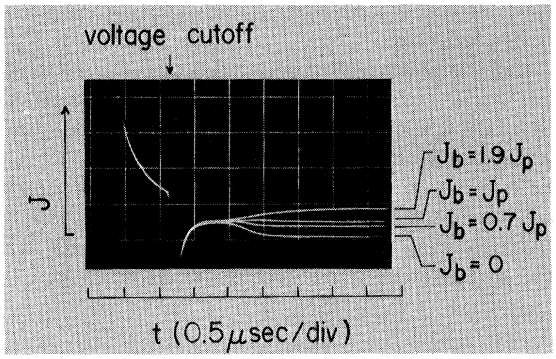

FIG. 6. Current traces for various biasing voltages, represented here by the corresponding ultimate bias currents J_b. The bias voltage in the form of a long low voltage pulse is applied shortly after cutoff of the primary voltage. A common plateau in the current persists for all bias voltages until the flux decays sufficiently to allow the sample to return to its Ohmic condition. The currents then approach their Ohmic bias levels at different rates.

toelectric contribution to the attenuation is clearly demonstrated. For $\gamma = 0$ there is pure lattice attenuation with $\alpha_n = -\alpha_l$. For $\gamma = 4$ the net attenuation is almost zero, indicating that the acoustoelectric gain is almost compensating the lattice attenuation. At $\gamma = 5.5$, $\alpha_n = \alpha_0\gamma - \alpha_l > 0$, and there is small net gain giving slight growth of the flux.

The range of signal over which exponential variation is followed is dependent on the growth (attenuation) rate, being roughly one order of magnitude for the case of growth. The acoustic intensities here are about seven orders of magnitude greater than at thermal equilibrium, from estimates based on the Debye equilibrium acoustic intensity and the strength of Brillouin scattering.[2]

We shall make a brief diversion here to discuss (a) the shape of the bias current during attenuation, (b) the corresponding conditions of field inside the flux domain, and (c) the method of determining the parameter γ. A superimposed set of current pulses is shown in Fig. 6 for various values of bias J_b. There is an initial current transient, common to all the pulses, which represents a portion of the drop in current during flux growth. Consider first the curve for zero bias, $J_b = 0$. After the voltage pulse is cut off at the indicated time, the current drops sharply (with a negative overshoot which is a remediable circuit effect) to a plateau which lasts for about a microsecond before decaying to zero. This persistent current is the consequence of the acoustoelectric attenuation of the flux, as described elsewhere.[28,29] The current is produced by the transfer of momentum[30] from the acoustic flux to the electrons; this is the inverse of the amplification process. To a fairly good approximation[29] the persistent current density during the plateau is given by $J_p = nev_s$; this can be seen to be independent of our small variations in J_b. The acoustic flux is decaying even during the time the current remains in the plateau.[28] The persistent current begins to fall off to zero only when the acoustic intensity becomes sufficiently weak that the rate of momentum transfer from the flux to the electrons can no longer sustain an electron drift velocity equal to v_s. The plateau current, designated J_p, is very useful for determining the quantity nev_s in $\gamma = J_b/nev_s - 1$. If the sample is not homogeneous and n varies as a function of the position along the sample through which the attenuating domain is moving, this can be revealed through a variation of the plateau J_p with time.[29]

The variable bias current alters the acoustoelectric part of the attenuation, and hence the net rate at which the flux decays,[28] and in turn affects the related rate at which the current approaches its externally determined steady-state value J_b. If we make $J_b = J_p$, which corresponds to $v_d = v_s$, the acoustoelectric interaction given by $\alpha_0\gamma$ is zero, and the flux decays by lattice attenuation alone. In this case, the presence of the flux is undetected in the current, which undergoes no transient change as the flux decays. For $J_b > J_p$, e.g., at $J_b = 1.9\,J_p$ in Fig. 6, we note that the current *rises* to its steady-state value of J_b. Here there is still *net* attenuation of the flux, even though the acoustoelectric interaction itself is now in the amplifying stage and the electrons are losing momentum to the flux. The excess resistance decreases as the flux decays and causes the current to *rise* to its final, steady-state value. The prolonged rise time of the current here indicates that the net rate at which the flux attenuates is very weak.

The dc electric field inside the domain during the various stages in Fig. 6 is determined by the rate of acoustoelectric gain (or loss) of energy. From an extrapolation of the small-signal momentum-conservation relationship, the field at a position x is taken to be

$$E(x) = \frac{v_d}{\mu} + \sum_f \frac{\alpha_0\gamma\phi(f)}{nev_s}\,, \tag{4}$$

where $v_d/\mu = E_0$ is the Ohmic contribution to the field. $\Delta E(x) = E(x) - E_0$ is the deviation of the field from its Ohmic value. It arises from the exchange between the electrons and amplified flux, of phonon momentum density ϕ/v_s, which is multiplied by the appropriate frequency-dependent gain coefficient $\alpha_0\gamma$ and summed over all frequencies. The excess field in the domain is very high and positive during strong-flux growth. When the applied voltage is cut off, γ drops down through zero to small negative values, where attenuation sets in. Correspondingly, ΔE decreases, passes through zero, and becomes negative. In the weak-flux regime,

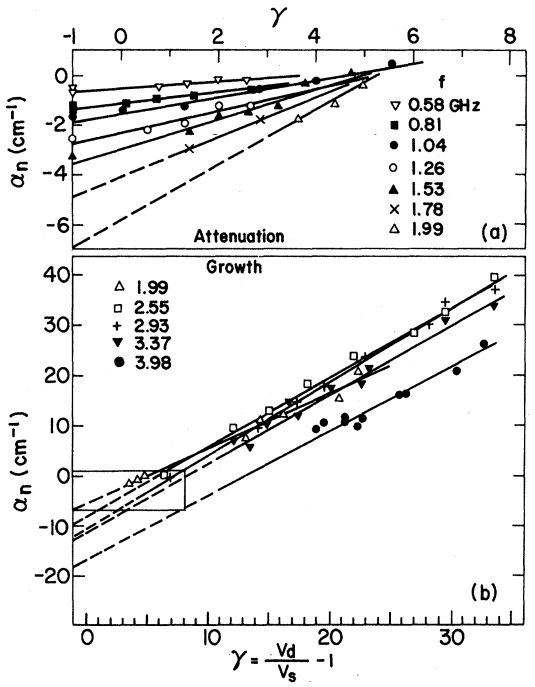

FIG. 7. Plots of α_n vs γ obtained by the methods discussed in the text. The data in part (a) were obtained primarily during flux attenuation. The data in part (b) were obtained during growth. The rectangular box in part (b) indicates the location of the data in part (a).

ΔE becomes small, with its sign determined by γ.

B. Determination of Coefficients α_0 and α_l

Figure 7 shows α_n vs γ for various frequencies, (a) at $f < 2$ GHz, mostly during attenuation ($\alpha_n < 0$), and (b) at $f \gtrsim 2$ GHz, mostly during flux growth ($\alpha_n > 0$). The slope of each line gives α_0 at the particular frequency, and the intercept at $\gamma = 0$ gives α_l. There is a congested intersection of lines in Fig. 7(b) because α_0 goes through a broad maximum near 3 GHz.

The variation of α_0 with frequency is shown in Fig. 8. The scale for α_0 is given in units of cm^{-1}; it can be converted to units of sec^{-1} by multiplying by $v_s = 3.35 \times 10^5$ cm/sec. It represents here the gain coefficient for acoustic energy density and not amplitude of the sound waves. Uncertainty in the determination of α_0 is estimated to be $\pm$ 20%. The frequency bandwidths over which the data points are effectively averaged are indicated by the resolution bars at the bottom of the figure. The resolution is affected by the 20% bandpass in optical wavelength λ_0 and by the effective collection aperture of the detector. No substantial variation was found in the region below 1 GHz between attenuation measured with a $4\frac{1}{2}°$ aperture cone and with a 2° cone.

Figure 9 contains the frequency dependence of the lattice attenuation $\alpha_l = 1/\tau_p v_s$, where τ_p is the phonon lifetime and v_s is the appropriate sound velocity. The data are given both for the transverse waves ($\alpha_l \propto f^{1.8}$) obtained from the extrapolation of the α_n-vs-γ data, and for the piezoelectrically inactive longitudinal waves ($\alpha_l \propto f^{1.3}$) obtained from direct attenuation studies of the reflected domain after mode conversion at the anode. In converting from α(cm^{-1}) to α(sec^{-1}) the appropriate sound velocity must be used. We note that the attenuation is greater for the LA flux, but the frequency dependence is stronger for the TA flux.

For comparison with our data, we also include in Fig. 9 the only available data from the literature for conventional measurements utilizing microwave-injected waves. The lone datum point of Keller and Abeles[31] at 0.63 GHz at 300 °K for the fast TA wave measured in semi-insulating GaAs falls close to the present data. The data of Bobylev and Kravchenko[32] (shown by the triangles) are for the LA waves in the [110] direction and are limited to the frequency range 20–200 MHz. Their data, for a sample with resistivity of 0.014 Ω cm and hence two orders of magnitude more free carriers than in our material, show an $f^{1.6}$ dependence and are reasonably compatible with our data, which hint at a smaller frequency dependence at the higher frequencies. The Bobylev-Kravchenko data for an

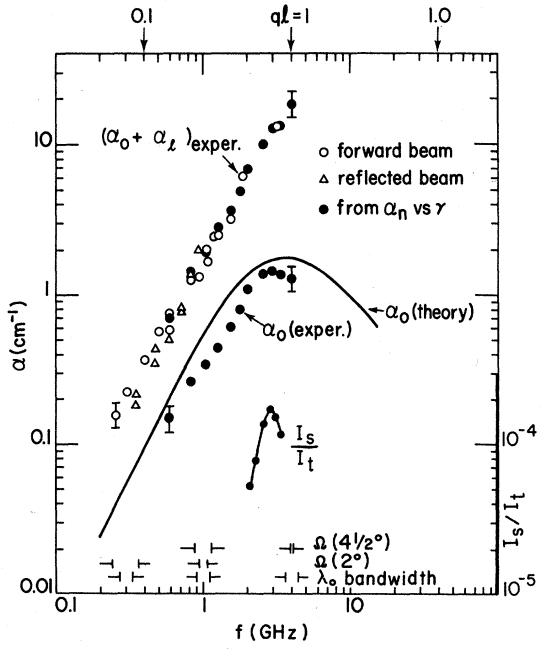

FIG. 8. Experimentally determined data for $\alpha_0 + \alpha_l$ and α_0 as a function of frequency. Also shown is the theoretical curve for α_0 obtained with the sample parameters given in the text. A typical experimental Brillouin-scattering ratio I_s/I_t in the vicinity of the frequency of maximum net gain is also shown for the small-signal gain regime.

unspecified TA wave (not shown in Fig. 9) fall among their LA data points and are not compatible with our data, possibly because they may represent the slow rather than the fast TA waves.

The magnitude of the total attenuation for the shear waves, $\alpha_n = -(\alpha_0 + \alpha_l)$ at $\gamma = -1$, or zero bias current, is shown in Fig. 8. Combined data are presented from the forward and reflected domain, and from extrapolation of α_n vs γ, for various runs in different portions of the sample, to demonstrate the scatter obtained by the present methods. The lattice attenuation exceeds the acoustoelectric attenuation for $J_b = 0$. The dominance of lattice attenuation becomes more marked at the higher frequencies.

The frequency bandwidth of the amplified flux itself is much narrower than the bandwidth of the acoustoelectric gain. The exponential dependence of I_s/I_t on $\alpha_0 \gamma t$, is, of course, responsible for the narrowing of the acoustic bandwidth. This can be seen from comparison of I_s/I_t data in Fig. 8 with the α_0 data. The I_s/I_t data were taken at $\gamma = 35.6$ for a growth time of 1.2 μsec. At this value of γ, the gain appreciably exceeds the lattice attenuation, and the frequency of maximum *net* gain should be close to the frequency of maximum gain. This is sharply determined by the I_s/I_t data as 2.9 GHz and is consistent with the much broader maximum for the α_0 data.

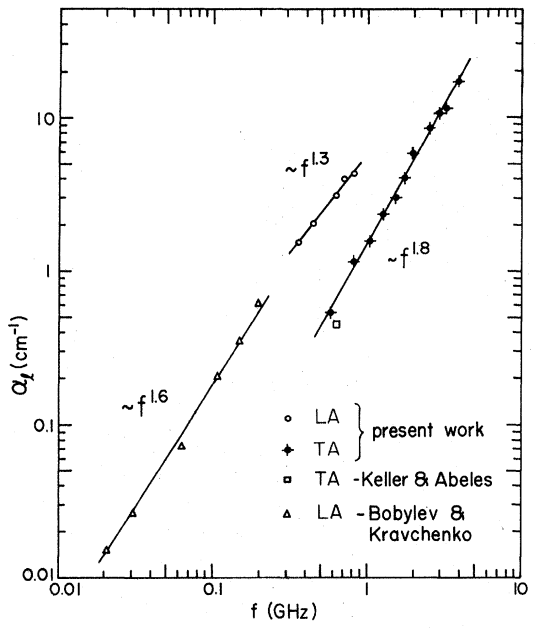

FIG. 9. Attenuation α_l for both the fast TA wave as obtained from the $\gamma = 0$ intercepts in Fig. 7 and the LA wave as observed in reflection. The frequency dependencies of the attenuation data are indicated. Also shown are some data available from conventional attenuation studies of microwave-injected flux from Refs. 31 and 32.

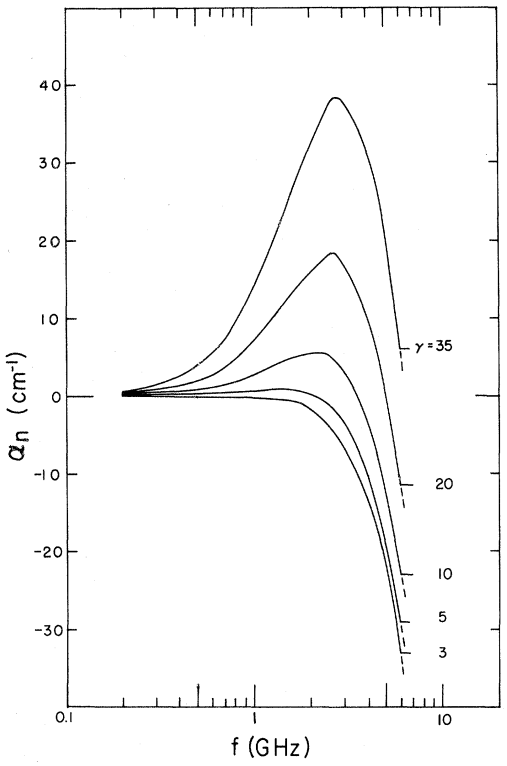

FIG. 10. Calculated plot of α_n vs f (using experimental data for α_0 and α_l) for several values of γ illustrating the shift of the frequency of maximum net gain to lower frequency as γ decreases, simply due to the frequency dependence of small-signal parameters α_0 and α_l.

In Fig. 10, we illustrate the sensitivity of the frequency dependence of the net gain to the value of γ. The frequency dependence of α_n for various values of γ was calculated with use of the α_l (TA) line in Fig. 9 and the α_0 calculated curve of Fig. 8 (multiplied by 0.8 to fit the data points). At large values of γ, the peak in α_n is close to 2.8 GHz. As γ is decreased, the peak in α_n downshifts considerably, approaching an $f \approx 1$ GHz at $\gamma \approx 5$. Flux growth can continue at low frequencies for $\gamma \approx 3.5$, below which no growth should occur. This calculation demonstrates the effect of the lattice-loss term on the net-gain spectrum and has some interesting consequences with regard to the evolution of domain shape and the frequency distribution of flux within the domain. If the domain is initially built up at high γ, the peak of the acoustic flux should be close to f_m. The flux buildup generally forces the current down to a saturation value of v_d close to v_s. In the wings of the domain, where the flux is relatively weak, the gain may still be given by the small-signal expression $\alpha_0 (v_d/v_s - 1)$. Here then, the initially amplified high frequencies must attenuate. Thus, the wings of any broad domain will be naturally clipped off when the current drops to the saturation value, as was observed by

Spears and Bray.[33] Within the intense core of the domain, the acoustoelectric gain cannot be expected[2,19-22,34] to be given by the small-signal theory and the implications of Fig. 10 need not be applicable.

C. Comparison with Theory

a. Acoustoelectric coefficient. The theoretical curve for α_0 is shown in Fig. 8; it lies about 20% above the experimentally determined values. Since the parameter ql is of order unity near f_m, the theoretical curve had to be calculated from the general expression developed by Jacoboni and Prohofsky.[13] The latter coincides with the $ql \ll 1$ gain curve at lower frequencies where $ql \leq 0.3$.

An important assumption in the theory is that the electron momentum relaxation time is energy independent. The effect of an energy-dependent relaxation time on the gain has been calculated recently by Jacoboni and Prohofsky.[35] The effect is quite appreciable and can more than encompass the present discrepancy. For impurity scattering dominant, the gain at the peak should be increased by about 70%; for acoustic-phonon scattering, it should be decreased by a factor of $\frac{1}{4}\pi$. These corrections are important only for $ql \approx 1$. Unfortunately, in GaAs at room temperature, polar optical-phonon scattering should be very important, so we can not assess if the proper correction of the theory would increase or decrease the discrepancy with experiment.

Another source of error is the considerable uncertainty in the parameters that appear in the theoretical expression for α_0. Thus the electromechanical coupling constant K^2 is taken[2] equal to $3.7\times10^{-3}\pm10\%$. Furthermore, n was determined from the persistent current plateau $J_p = nev_s$, but we observed about a 20% fluctuation in J_p, depending on the position of the domain in the sample, when the voltage pulse is cut off. This fluctuation represents the inhomogeneity in n of the material. From the average value of J_p, we obtained $n = 5\times10^{14}$ cm^{-3}, which taken together with the conductivity, yields a value for the mobility of 9800 cm^2/V sec. The latter is at least 10% higher than has been reported in the literature from Hall measurements on comparable material and about 5% higher than the limit of 9300 cm^2/V sec estimated for polar scattering.[36] In the absence of more homogeneous material, it is difficult to determine these fundamental parameters with any greater certainty.

b. Lattice attenuation. From our results on the lattice attenuation at 300 °K of ultrasonic flux with frequencies near 1 GHz, two features emerged: (i) The frequency dependence of the attenuation in the available range of measurement is $f^{1.8}$ and $f^{1.3}$ for the TA and LA modes, respectively, and (ii) the attenuation is appreciably greater for the LA than for the TA modes. We have already indicated that there are insufficient data from conventional measurements on GaAs to permit adequate comparison. However, we shall consider how our results compare with available data for other materials, and how they fit in with existing theory.

The lattice attenuation[37] of the ultrasonic flux is ascribed to its interaction with the thermal phonons in a three-phonon process. Simple theoretical predictions for the frequency dependence of α_l are available for extremes of the parameter $\omega\tau_{th}$, where ω is the angular frequency of the ultrasonic waves and τ_{th} is the relaxation time of the thermal phonons with which the sound waves interact. Thus for $\omega\tau_{th} \gg 1$, α_l can vary approximately as ω. For $\omega\tau_{th} \ll 1$ the relevant theory is that of Akhiezer,[38] or one of its many modifications[37,39] according to which α_l may vary as $\omega^2\tau_{th}/(1+\omega^2\tau_{th}^2)$. The proportionality constant includes various complicated averages[39,40] of the Grüneisen numbers for the thermal-phonon modes. For the transition range, where $\omega\tau_{th} \approx 1$, more complicated expressions have been derived[41] for the attenuation.

A prerequisite for the analysis of the attenuation is the determination of an appropriate average of τ_{th} over the relevant thermal-phonon modes, taking into account their various scattering mechanisms. Instead, τ_{th} is commonly estimated from the thermal conductivity on the dubious[42] assumption that the phonons important in determining thermal conductivity are the same as those interacting with the ultrasonic flux. For GaAs at 300 °K, the thermal conductivity yields[40] $\tau_{th} = 8.2\times10^{-12}$ sec. Thus, at $f = 1$ GHz, $\omega\tau_{th} = 0.05$ and the $\omega\tau_{th} \ll 1$ limit should apply. Using this τ_{th}, Lewis[40] has estimated an attenuation coefficient $\alpha_l/f^2 = 5.2$ cm^{-1}/GHz^2 for longitudinal waves in the [100] direction. This is not expected[40] to differ much for the LA modes in the [110] direction. At $f = 1$ GHz the magnitude of α_l is in quite good agreement with our measured value (see Fig. 9). However, the appreciable difference between the theoretical and the observed frequency dependence of the attenuation renders the significance of such agreement suspect.

Before commenting further on the discrepancy in the frequency dependence for both TA and LA modes, we note that a survey of other materials reveals general departures from an f^2 dependence at 300 °K in the GHz frequency range. Attenuation close to f^2 has been reported for Ge and in some alkali halides,[40,43] but the data are extremely meager and in a relatively low-frequency range, $0.01 > f > 0.2$ GHz for the alkali halides, and $0.04 < f < 0.5$ GHz in Ge for composite data[37] of various investigators. Otherwise, various studies reveal an appreciably slower than f^2 dependence at 300 °K. Thus, for Si,[37] $\alpha_l \propto f^{1.7}$ in the range

$0.2 < f < 0.8$ GHz; for ZnO,[44] it is $f^{1.6}$ for $0.5 < f < 1$ GHz; for CdS,[45] it is $f^{1.46}$ for $0.1 < f < 0.5$ GHz; and for Al_2O_3,[46] it is $f^{1.7}$ for $0.3 < f < 3.0$ GHz.

The above departures from the theory have received relatively little attention in the literature. Experimental data over a much wider range of frequency would be welcome to check for a possible transition near $f \approx 1$ GHz, from an f^2 towards an f dependence. Thus, if $\omega\tau_{th} \approx 1$ in this frequency range, we could understand the slower than f^2 dependence of the attenuation. However, this would require $\tau_{th} \approx 1/\omega = 1.6 \times 10^{-10}$ sec at 300 °K, some 20 times longer than the value obtained from the thermal conductivity.

A mechanism for giving a deviation from an f^2 dependence in the $\omega\tau_{th} \ll 1$ regime is a strong frequency dependence for τ_{th} itself. It has been pointed out by Miller[41] that if $\tau_{th} \propto \omega^n$ and $n < 3$, then the main contribution to the integral for α_l, which contains $\tau_{th}(\omega)$, comes from thermal phonons with $\hbar\omega \approx kT$, and yields the Adhiezer frequency dependence. For $n > 3$, the thermal phonons of lower frequency are important; specifically for $n = 4$, which applies for point defect or mass difference scattering,[37] the attenuation would vary as $f^{7/4}$. However, analysis[47,48] of thermal conductivity in GaAs at room temperature seems to require umklapp scattering (an $n = 2$ process), but no contribution from mass difference scattering which is important at low temperatures. This again raises the question whether the τ_{th}'s appearing in thermal conductivity and in lattice attenuation are effectively determined by the same or a different distribution of thermal phonons and scattering processes.

Our observation that the attenuation for [110] LA modes is stronger than for [110] TA modes is consistent with conventional measurements in GaAs,[31] Ge,[39] and Si.[39] Comparative attenuations are not easily obtainable from theory. Mason and Bateman[39] arrived at the empirical conclusion that τ_{th} is about twice as long for LA as for TA interactions. The supposition is made[39,40] that the two types of modes may interact with different groups of thermal phonons which have a distribution of τ_{th}'s. However, other factors (such as sound velocity and functions of the Grüneisen constants) in the expression for the attenuation are also different for TA and LA modes. A recent analysis by Kishore[49] gives α_l greater for LA than TA modes in Ge and Si, in fair agreement with experiment, without making arbitrary assumptions about relative τ_{th}'s for these modes.

V. ANOMALOUS ATTENUATION AND FREQUENCY-CONVERSION EFFECTS IN STRONG-FLUX REGIME

A. Evidence for Frequency Up-Conversion

Anomalous attenuation in strong flux, just after cutoff of the applied voltage pulse, was noted for region E of Fig. 4. The anomaly consists of (a) the relatively slow initial attenuation of the high-frequency flux (e.g., at 3.1 and 3.6 GHz), before it achieves its expected rapid lattice attenuation, and (b) the rapid initial attenuation of the low-frequency flux (e.g., at 1.04 and 0.59 GHz), before it settles into its expected slow attenuation. At intermediate frequencies [e.g., 1.53 and 1.99 GHz in Fig. 4(d)], one can see a more complex pattern of transition in attenuation rate, from slow to fast to slow again, as the flux intensity decreases.

The simplest interpretation of these effects is that, in addition to acoustoelectric and lattice attenuation, there is a rapid transfer of energy from low to high frequencies in the strong-flux regime. Such an up-conversion process would account simultaneously for the too-rapid decay of the low frequencies[50] and the retarded decay of the high frequencies. In the latter case, the inflow of up-converted flux would partially compensate for the ever-present rapid lattice attenuation, which would prevail only as the up-conversion process dies out. At intermediate frequencies, flux may be transferred in from below by up-conversion and also transferred out to higher frequencies, with the balance between in- and outflow varying as the flux distribution changes. Thus in Fig. 4(d) we note at the intermediate frequencies the following sequence: There is initially a slow attenuation between 3.8 and 4.5 μsec when inflow from lower frequencies may be dominant; then there is a more rapid attenuation at $4.5 < t < 5.5$ μsec when outflow may become dominant. The latter seems to coincide with the slowing down of the attenuation at the low frequencies, perhaps as they cease to function as a source for the higher frequencies. Finally, the attenuation slows down again in region F, where the weak-flux acoustoelectric and lattice attenuation take over, as discussed in Sec. IV.

A close examination and comparison of the attenuation curves for the low frequency $f = 0.59$ GHz reveals a rather interesting detail, namely, that the transition from the fast to the normal, slow, decay occurs at the very different signal intensities of $I_s/I_t \approx 3 \times 10^{-4}$ in Fig. 4(b), of $\approx 2 \times 10^{-3}$ in 4(c), and of $\approx 10^{-2}$ in 4(d). Thus the transition in decay rate appears not to depend on the intensity of the low-frequency flux; rather it appears to correlate with the time when the signal intensity of several of the higher frequencies falls below some specific level; note, e.g., the correlation with the time at which I_s/I_t falls below $\approx 10^{-4}$ for $f = 3.09$ GHz in all the cases shown. Thus the fast decay of low frequencies by up-conversion seems to be more dependent on the presence of some critical level of flux at the higher frequencies to *stimulate* the

process, than upon its own intensity level. This suggests that up-conversion at low frequencies is not taking place by second-harmonic generation but by interaction and mixing with the high-frequency flux.

We may relate this interesting observation in the nature of the strong nonlinear interaction in the piezoelectric semiconductors.[4-6] The effective third-order elastic constant governing the nonlinear interaction is dominated by the electron-lattice interaction between bunched electrons and piezoelectric fields which greatly exceeds the contribution from the lattice anharmonicity.[5] The electron-lattice interaction is frequency dependent, with a maximum at $2\pi f_m \approx (\omega_c \omega_D)^{1/2}$. This frequency dependence of the acoustoelectric interaction is also present in the relevant theoretical expressions[5,6,23] for the mixing interactions. Although the conditions in the intense core of the domain are complicated, it appears plausible that those mixing interactions may be favored which involve the participation of flux near f_m for which the interaction strength may be dominant. Thus the involvement of the high-frequency flux may be required for the efficient up-conversion of the low frequencies, possibly through the production of sum and difference frequencies. As the high-frequency flux dies out, the nonlinear attenuation of the low frequencies may cease. This suggestion of a possible catalytic effect of flux near f_m on the nonlinear interactions of flux at much lower frequency should be susceptible to experimental test and analysis under the simpler conditions attainable with injected coherent flux.

Before proceeding with further discussion of frequency conversion and its implications, we shall consider first what alternative explanations there might be to the anomalous attenuation of the strong flux.

B. Consideration of Alternative Explanations

Three conceivable alternatives are that the strong-flux anomalies are caused by changes either in the lattice attenuation, or in the acoustoelectric coefficient, or in the conditions of Brillouin scattering and its ability to describe accurately the spectral distribution of the flux.

For lattice attenuation to be responsible for the anomaly, it would be necessary for α_l to be transformed in strong flux so as to become very much weaker at the high frequencies and much stronger at the low frequencies. Such a drastic reversal in the frequency dependence of α_l is difficult to imagine. On the other hand, it has been claimed in several theoretical analyses[19-22,34] that the acoustoelectric coefficient is appreciably modified in strong flux. It is thus conceivable that the initial rapid attenuation at low frequencies could be due to a strong enhancement of the acoustoelectric attenuation at these frequencies by its transformation in the strong flux. However, no change in the acoustoelectric interaction can explain the retarded attenuation at high frequencies. There, the lattice attenuation is dominant (if it is at the same strength as for weak flux). Any contribution from acoustoelectric attenuation can only further *increase* the attenuation, *not greatly decrease* it below the expected value for lattice attenuation. Thus a shift of the acoustoelectric gain curve cannot, by itself, account for all the details of the anomalous behavior.

Finally, we consider the Brillouin-scattering effect. In intense flux, multiple scattering enters as a factor that can distort the analysis of the acoustic spectrum. Multiple scattering is most likely to involve the lower acoustic frequencies for which the signal I_s/I_t becomes very large. As an example of possible distortion in the information, three successive scatterings from a combination of off-axis low-frequency phonons can simulate a single scattering event from a high-frequency phonon. Thus the observed signals for the high frequencies can contain a component derived from such multiple-scattering events. Some evidence for the existence of such a contribution was obtained, and it is described and analyzed in the Appendix. However, we can rule out multiple scattering as a major factor in the present anomaly on the grounds that multiple scattering is a higher-order process than single scattering, and as such its contribution to the scattering signal for the high-frequency flux would have to decay much faster than the signal for low frequencies. This is in contradiction with the observation in Fig. 4 that the initial decay of the high-frequency signal is actually appreciably slower than that of the low-frequency signal. In any case, it is difficult to see how multiple scattering could explain the anomalous fast decay of the low-frequency signals. Note from Fig. 4 that the fast low-frequency decay occurs both at signals I_s/I_t of $\approx 10^{-3}$ in (b) and at $\approx 10^{-1}$ in (d). In the latter case the fast component of the decay disappears even when the scattering signal has dropped to only $\approx 10^{-2}$. Thus, the anomalous fast decay does not seem to be strongly dependent on scattering strength *per se*, and is present even when multiple scattering can be ruled out.

The various observations and qualitative arguments strengthen previous conclusions that the frequency-conversion processes are very strong in intense flux and capable of playing a dominant role in determining the evolution of the spectrum in acoustoelectric domains. We do not imply here that the acoustoelectric gain in strong flux is not appreciably altered from that in weak flux, but only that the major factor in the evolution of the strong-flux spectrum is the frequency-conversion inter-

action within the amplified flux.

We did attempt to determine the importance of the acoustoelectric attenuation in the strong-flux condition. The approach was to observe the effect of varying the bias, and hence the acoustoelectric contribution, on the anomalous attenuation. The results are shown in Fig. 11, where the complete evolution of the flux is presented at representative low (1.04 GHz) and high (3.03 GHz) frequencies for three bias conditions: $J_b = 0$, $J_b \approx J_p$, and $J_b > J_p$. For these biases, it is reasonable to assume that the gain factor γ, whether given by $v_d/v_s - 1$ or not in the strong-flux domain, is varied at least from negative to positive and hence that the acoustoelectric interaction is changed from attenuation to gain. In all three cases, there is still *net* attenuation over the whole observable frequency range because of the dominance of the lattice attenuation. We see that there is little difference in the decay patterns for $J_b = 0$ and $J_b \approx J_p$. At $J_b > J_p$, the rate of decay of the flux at both frequencies decreases considerably, but the anomalous features (fast initial decay at low frequency and slow initial decay at high frequency) are still observable. Thus the conclusion can be drawn that the essential features of the anomalous attenuation in strong flux are not altered by the variation in the magnitude and sign of the acoustoelectric effect, and hence the latter (as narrowly defined in the Introduction) cannot be the dominant factor in the anomaly. The much longer persistence of the flux at both frequencies for $J_b > J_p$, when the acoustoelectric gain is positive, does indicate, however, that the acoustoelectric gain still has considerable influence on the evolution of the flux.

C. Transition from Down- to Up-Conversion

The observation of the transition from down-conversion of the frequencies of the acoustic flux during growth, to up-conversion during attenuation, poses interesting questions as to how and when the transition takes place. We would expect both up- and down-conversion processes to occur concurrently through mixing of all the frequencies; i.e., there seems to be no obvious selection rule mitigating against up- or down-conversion whose reversal can be effectuated to provide the transition. Therefore, it seems most reasonable that the conversion observed at any time represents a *net trend*, the direction of which may depend on the interplay of the acoustoelectric, lattice attenuation, and frequency-mixing processes. As the spectral distribution of the flux changes or the applied field is shut off, the relative contributions of these processes can change and thus provide a transition in the net conversion rate. Below, we shall attempt to fill in this picture in rather broad strokes.

Consider first the flux-growth regime. When the field is on, energy is pumped into the electrons and transferred via the acoustoelectric effect to the acoustic flux. Into which band of acoustic frequencies most of the energy is pumped in strong flux, whether near f_m or eventually at much lower frequencies, is one of the points of contention on which we shall comment later. The main point now is that the flux at any frequency is observed to be either approaching steady state or still growing rapidly; at no frequency is the flux observed to be attenuating before the field is shut off. This means that enough energy is supplied to all observable frequencies to more than compensate lattice losses. Irrespective then of where the energy is pumped in, it appears to be rapidly spread throughout the spectrum by frequency mixing. The observation of continued growth of flux at low frequencies while the flux at higher frequencies tends to saturate may be attributed to the frequency dependence of the lattice attenuation. The strong lattice attenuation at high frequencies ($\alpha_l \propto f^{1.8}$) mitigates against the storage of the high-frequency flux and thus against observation of up-conversion to frequencies greater than f_m. Much more flux can be stored at low frequencies, e.g., at 0.6 GHz where the phonon lifetime (as determined by the lattice attenuation) becomes greater than the

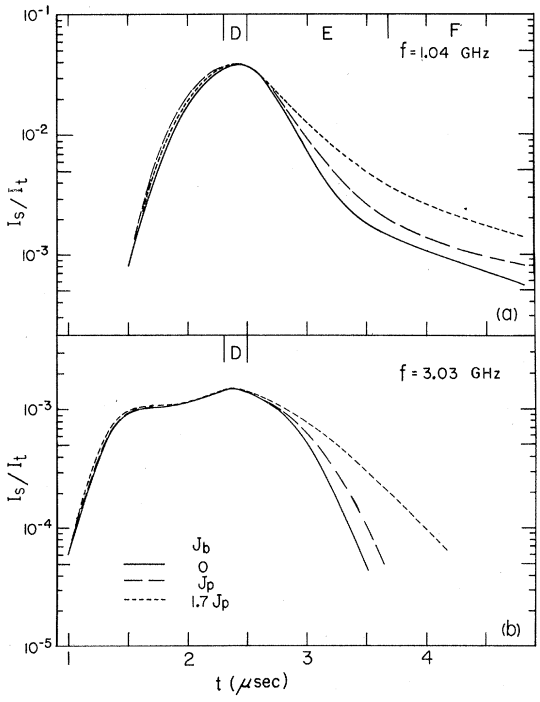

FIG. 11. (a) I_s/I_t for a low frequency for three values of bias current. (b) I_s/I_t for a high frequency for the same three values of bias. These data illustrate the dependence of the strong-flux attenuation anomaly on sign and magnitude of the acoustoelectric gain.

transit time of flux through a 2-cm-long sample. Thus, as long as the energy input into the traveling domain of flux continues, buildup of the low-frequency end of the spectrum can continue, thus thwarting the achievement of a steady state, and at the same time producing a continuous shift of the peak of the spectrum to lower frequency.

A turning point occurs when the applied voltage is shut off and the energy input into the flux ceases. The combined attenuation processes are strongest at high frequencies. If frequency mixing is strong, we expect the low-frequency flux to be dragged down along with the high frequencies. Thus the former is forced to decay too rapidly while the decay of the latter can be delayed. We make no pretense of explaining the relative rates of decay of the flux at the various frequencies, e. g., why the low frequencies decay initially faster than the flux at high frequency. This would require a detailed knowledge of the frequency-mixing rates and their dependence on the instantaneous form of the spectral distribution. Very broadly, then, we have depicted the transition from down- to up-conversion as a reversal in a net trend when the applied voltage is shut off. The trend when the voltage is shut off may also depend on the spectral distribution at that instant. For example, Spears[2] and Robinson and Butler[51] have observed evidence for continued down-conversion for a brief interval after the voltage is shut off. Conceivably, this could happen if the voltage is shut off relatively early, before the low frequencies have time to build up strongly.

D. Comment on Frequency Downshift of Acoustoelectric Gain

No evidence has been adduced for the frequency downshift of the acoustoelectric gain in strong flux, except for the observed fact of the downshift in the peak of the acoustic spectrum. If the downshift in the gain were indeed a dominant factor in the evolution of the spectrum, it would have to provide not only the visible flux growth at the low frequencies after the current drops close to its saturation value, but also the considerable energy which would have to be spread up to the higher frequencies through frequency mixing to prevent their disappearance by lattice attenuation if the gain at those frequencies thereby becomes reduced in strong flux. It is not at all clear that any of the theories,[19–22] based on a single-mode model, predict such a drastic frequency downshift as is actually observed, or that they are in fact relevant to the domain with its multimode structure. At this stage, it seems more reasonable that the gain in strong flux is not shifted drastically below the initial f_m. An argument favoring this viewpoint is based on the various observations that the peak field in the domain always appears to saturate early, at about the same time that the flux near f_m tends to saturate. This puzzling early saturation of the field has been reported in many different types of experiments in both GaAs [2,52] and CdS.[15,53,54] If Eq. (4) is relevant in strong flux, the excess field in the domain is proportional to $\sum_f \alpha_0 \gamma \phi(f)$. Then the field is determined not just by the flux, but also by the frequency-dependent weight factor $\alpha_0\gamma$, which determines the rate at which momentum is transferred to the flux. Thus a saturation of the field requires a saturation of the product of flux and gain coefficient. However, if the gain shifts drastically to lower frequencies, the high-frequency flux would be weighted by a presumably reduced gain and would no longer contribute to the field. Only the appropriately weighted low-frequency flux would then contribute. But, in spite of the peaking of the flux at low frequency, Spears[2] has shown that most of the integrated acoustic energy remains near high frequency. It is difficult to see how the domain field could saturate and stay constant if the gain did indeed shift down drastically. Our conclusion, that frequency mixing rather than drastic changes in the spectrum of the acoustoelectric gain is the most important factor in the evolution of the strong-flux spectrum, is not necessarily in contradiction with the acoustoelectric theories,[19–22] since none of them have incorporated both effects and tried to evaluate their relative contribution for the case of a domain with its multitude of modes.

VI. SUMMARY

Three types of phonon interactions were studied in acoustoelectrically amplified domains in GaAs. These interactions, separated where possible by virtue of their different dependence on current or acoustic intensity, include (a) the acoustoelectric interaction, (b) ordinary lattice attenuation, and (c) the phonon-phonon interaction giving frequency mixing and conversion of acoustoelectrically amplified flux. Where the interactions were *not* fully separable, as in strong flux, the role of each in determining the observed phenomena was assessed. The basic data were the measurement of the growth and attenuation (particularly the latter) of the acoustic flux as a function of frequency, by means of Brillouin-scattering experiments.

In the weak-flux regime, where only the first two interactions are important, quantitative data could be obtained in the range 0.3–4.0 GHz, of the frequency dependence of these two interactions for fast [110] shear waves. Comparison with acoustoelectric theory in the range $ql \approx 1$ gave quite fair agreement within the uncertainties in the material parameters, and within the approximations in the theory. The lattice attenuation for longitudinal and transverse waves was found to vary as $f^{1.3}$ and

$f^{1.8}$, respectively, well below the expected f^2 variation. We believe that the technique of Brillouin scattering from acoustoelectrically amplified flux should prove useful for more systematic study of the lattice attenuation of high frequencies whose decay is too rapid to be measured by the usual multiple-echo techniques.

The strong-flux regime is characterized by the onset of the third interaction, upon which is placed the predominant responsibility for the observed rapid evolution of the amplified acoustic spectrum. The evolution consists, during growth, of the previously documented spread of the acoustic energy to low frequencies, of the order of $\frac{1}{10}f_m$. This pattern is supplemented in the present study by the observation of the reverse trend during attenuation, i.e., the up-conversion of acoustic flux. The latter is deduced from the anomalous rapid decay of low frequencies and delayed attenuation of the high frequencies near f_m. Qualitative arguments based on various experimental tests were marshaled against the oft-proposed hypothesis that the evolution of the frequency spectrum of the flux could be accounted for *merely* by the transformation (downshift) of the frequency dependence of the acoustoelectric gain under strong-flux conditions. The evolution of the acoustic spectrum was discussed in terms of all three interactions. During growth, the acoustoelectric interaction pumps energy into the acoustic flux—probably mainly at frequencies near f_m. The frequency-mixing phonon-phonon interaction spreads the energy out over all frequencies. The lattice attenuation, varying as $f^{1.8}$, favors the storage of flux at the low frequencies, thus producing the downshift in the peak acoustic intensity. When the voltage is shut off, the strong lattice attenuation at high frequencies pulls along with it, via the phonon-phonon interaction, the flux at low frequencies. Thus, the phonon-phonon interaction in strong flux is pictured as tending to smooth out the sharper frequency-dependent effects of the other two interactions. The results suggested that the presence of the flux near f_m is important in stimulating the phonon-phonon interactions in the production of sum and difference frequencies. Although most of the complex observations are fitted into a consistent picture, the qualitative nature of the arguments at various points makes this picture still tentative.

ACKNOWLEDGMENTS

The authors wish to thank Dr. D. L. Spears for advice on the use of the Brillouin-scattering equipment and for fruitful discussions, V. Dolat for assistance with some of the measurements, and J. B. Ross for computer calculations. One of the authors (R. B.) acknowledges valuable discussions with Dr. N. Shiren. We gratefully acknowledge support by the NRL Sabbatical Study Program and the hospitality of the Physics Department, Purdue University, for E. D. P. during the year 1968-69 and the partial support of a Guggenheim Memorial Fellowship and the hospitality of the Clarendon Laboratory, Oxford, for R. B. during the year 1969-70.

APPENDIX

If multiple Brillouin scattering of the light beam occurs in strong flux, we can no longer attribute a given scattered-light signal to a particular acoustic frequency. Our particular concern here is with the situation when the Brillouin-scattering signals from flux of low frequencies becomes very strong. Then the possibility arises that multiple scattering from the low-frequency flux can contribute to, and thus falsify, the much weaker single-scattering signal for the high-frequency flux. We shall describe here an experiment which demonstrates this situation, and present an analysis for estimating the magnitude of such a multiple-scattering contribution.

A total scattering cross section $\sigma_T \gg \sigma_f$ can be defined by the relation $I_t = I_0 e^{-\sigma_T b}$, where I_0 is the transmitted light in the absence of any scattering and I_t is the light transmitted after depletion by scattering. Thus, whereas σ_f describes how much light is scattered into a given solid angle by phonons of a specific wave vector, σ_T describes how much light is scattered *out* of the incident beam by phonons of all possible wave vectors that can contribute to the scattering. The latter represents flux of different frequencies propagating at various angles within the amplified cone. The multiple scattering that is of concern here is for $\sigma_T b$ large, such that some of the light may be scattered more than once in passing through the sample. Such an effect can throw some scattered light back into I_t and make it too large; also, it can contribute falsely to the scattered-light signal I_s at the frequency of interest. The enhancement of I_t may be neglected here compared to the enhancement of I_s at f, for the case that the single scattering by the on-axis high-frequency f is weak, but the scattering by the on- and off-axis low frequencies is strong, and is mainly responsible for the multiple scattering. The fraction of the light scattered m successive times was shown by Spears[2] to be proportional to $(\sigma_T b)^m/m!$. An even number of scattering events will not give 90° rotation of the plane of polarization and will not contribute to I_s in our system of crossed polarizers. Therefore, it is mainly the effect of triple scattering ($m = 3$) by any allowed combination of phonons which concerns us here.

The main idea in the following experiment is to compare the scattering signal I_s/I_t at the high fre-

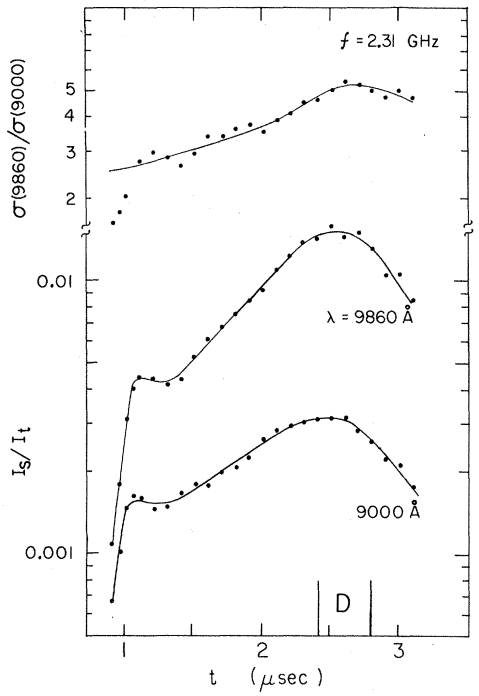

FIG. 12. I_s/I_t for two different wavelengths giving different scattering cross sections, illustrating that a part of the apparent growth at high frequencies is probably due to triple scattering by the much more intense low frequencies. At the top is shown the ratio of the scattering cross section at 9860 and 9000 Å. The fraction of triple scattering is analyzed in the Appendix.

quencies for different values of $\sigma_T b$ for a fixed distribution of flux. This can be achieved by varying the thickness b of the sample or comparing results on thick and thin samples. However, because of the very sensitive dependence of domain shape and acoustoelectric gain on resistivity and homogeneity of the material, it appeared too dangerous to make such comparative measurements. As an alternative, we resorted to varying the scattering cross sections σ_f and σ_T for a single sample by taking advantage of their dependence on wavelength λ_0 of the light[2,27] which takes the form $\sigma \propto p_{44}^2/\lambda_0^4$. Here p_{44} is the elasto-optic coefficient[55] and is itself wavelength dependent. By means of optical filters, two narrow bands at $\lambda_0 = 9000$ and 9860 Å were selected from the broad pulsed light source. The available light spectrum, determined by the GaAs sample and the Si detector, did not permit a larger wavelength spread. The work of Feldman and Horowitz[56] gives $p_{44} = 0.047$ and 0.065 at $\lambda_0 = 9860$ and 9000 Å, respectively, which yields the ratio $r_1 = \sigma_f(9860)/\sigma_f(9000) = 1.7$, a value somewhat smaller than the value $r_1 \approx 2.5$ which we measured in the weak-flux range at several acoustic frequencies. From the $\sigma^m/m!$ relationship, we can estimate the ratio of triple scattering at the two wavelengths to be $r_3 = (2.5)^3 \approx 16$. Thus even a small wavelength difference provides very appreciable discrimination of the multiple-scattering contribution.

In Fig. 12 we show the growth and decay curves of I_s/I_t for flux at $f = 2.31$ GHz and $b = 0.065$ cm, as measured at the two wavelengths. The ratio of the two scattering curves is also shown as a function of time. If there were no multiple-scattering contribution to the measured signal, the scattering ratio would be equal to r_1 and remain constant in time. The fact that it is increasing is an indication that there is a rising contribution from multiple scattering as the low-frequency flux builds up. The low-frequency flux is not shown here, but its buildup can be inferred from the earlier presentation and Fig. 4.

An estimate can be made from the data of Fig. 12 of the magnitude of the contribution from multiple scattering. Suppose the scattering cross section at 9860 Å is given by $\sigma = \sigma_1 + \sigma_3$ while that at 9000 Å is given by $\sigma' = \sigma_1' + \sigma_3'$, where σ_1 and σ_1' represent true contributions from once-scattered radiation (of 2.31-GHz frequency) and σ_3 and σ_3' represent contributions to I_s from thrice-scattered radiation (of any frequency combination). Let $r_1 = \sigma_1/\sigma_1'$ be the cross-section ratio for once-scattered radiation at the two wavelengths, $r_3 = \sigma_3/\sigma_3'$ be the ratio for thrice-scattered radiation, and $r = \sigma/\sigma'$ be the ratio of the combined scattered radiation. Algebraic manipulation of these expressions yields

$$\frac{\sigma_3}{\sigma} = \frac{1 - r_1/r}{1 - r_1/r_3}, \qquad \frac{\sigma_3'}{\sigma'} = \frac{1 - r/r_1}{1 - r_3/r_1}.$$

We take $r_1 \approx 2.5$ in the time interval 1.0–1.5 μsec, where there is a plateau in the two data curves. Earlier, at $t < 1$ μsec, the flux is changing very rapidly and the ratio is difficult to determine accurately. At the peak of the two curves we get $r \approx 5$. The triple-scattering contributions are then taken to be in the ratio $r_3 \approx (2.5)^3 \approx 16$. From these data, it turns out that triple scattering contributes about $\frac{1}{6}$ of the peak signal at 9000 Å, but about $\frac{2}{3}$ of the peak signal at 9860 Å. These results are not very sensitive to the exact values of scattering ratios r_1 and r_3 employed in the analysis. After allowance is made for the triple-scattering contributions, it appears that the single scattering for $f = 2.3$ GHz increases $\lesssim 50\%$ from its value at the plateau at $t \approx 1$ μsec to the time the voltage is shut off. Thus the high-frequency flux is much more nearly saturated after the first early buildup than originally appeared before the correction for multiple scattering.

These results suggest that in future studies in the intense-flux regime, very thin samples should

be used to avoid the systematic error from multiple scattering. Such errors in the analysis of the evolution of the high-frequency flux in the present experiments do not affect any of the conclusions drawn. In fact, the conclusion of the above analysis, that the high-frequency flux saturates more than was originally apparent, is consistent with the arguments given in the text relating the early saturation of the excess field in the domain and the high-frequency components of the flux.

---

†Work partially supported by the Advanced Research Projects Agency.

*Permanent address: Naval Research Laboratory, Washington, D. C. 20390

[1]For a review of acoustoelectric domain phenomena, see R. Bray, IBM J. Res. Develop. 13, 487 (1969).

[2]D. L. Spears, Phys. Rev. B 2, 1931 (1970); also, Ph. D. thesis (Purdue University, 1969) (unpublished).

[3]A. R. Hutson and D. L. White, J. Appl. Phys. 33, 40 (1962).

[4]A. R. Hutson, Phys. Rev. Letters 9, 296 (1962); N. Mikoshiba, J. Phys. Soc. Japan 20, 2160 (1965).

[5]B. Tell, Phys. Rev. 136A, 772 (1964).

[6]H. Kroger, Appl. Phys. Letters 4, 190 (1964).

[7]S. Zemon and J. Zucker, IBM J. Res. Develop. 13, 494 (1969). This paper contains a review of the frequency shift of the spectrum during growth, primarily in CdS.

[8]While the present manuscript was being written, a study appeared of the attenuation regime in CdS by A. Ishida and Y. Inuishi [J. Phys. Soc. Japan 29, 911 (1969)], containing a similar division into weak- and strong-flux effects and using variable bias voltage to separate acoustoelectric loss from lattice attenuation in weak flux. Ishida and Inuishi find much greater deviation of the acoustoelectric gain data from theory. In the anomalous strong-flux attenuation, they report only the too-rapid initial decay of low frequencies. Their assumption, that the anomalous rapid decay of strong flux is due to second-harmonic generation, is unsupported. Our study shows that the attenuation of strong flux is frequency dependent and much more complex. Finally, it must be noted that the light-scattering technique, as described by Ishida and Inuishi, differs substantially both from ours and from those reported by others for CdS. Specifically, they state (see Ref. 16 below) that the incident light beam is normal to the crystal surface, and that "effects of optical anisotropy were not taken into consideration" in analyzing the scattering of light. In this circumstance, for birefringent CdS, where optical anisotropy is important (see, e.g., Refs. 7 and 18), neither the frequencies nor the propagation direction of the acoustic flux in their experiments is properly determined.

[9]D. L. White, J. Appl. Phys. 33, 2547 (1962).

[10]D. L. Spears and R. Bray, J. Appl. Phys. 39, 5093 (1968).

[11]D. L. Spears, IBM J. Res. Develop. 13, 499 (1969).

[12]H. N. Spector, Phys. Rev. 127, 1084 (1962); R. K. Route and G. S. Kino, IBM J. Res. Develop. 13, 507 (1969).

[13]C. Jacoboni and E. W. Prohofsky, J. Appl. Phys. 40, 454 (1969).

[14]B. W. Hakki and R. W. Dixon, Appl. Phys. Letters 14, 185 (1969).

[15]W. Wettling and M. Bruun, Phys. Status Solidi 34, 221 (1969).

[16]A. Ishida and Y. Inuishi, J. Phys. Soc. Japan 26, 957 (1969).

[17]D. L. Spears and R. Bray, Phys. Letters 29A, 670 (1969).

[18]J. Zucker and S. Zemon, Appl. Phys. Letters 9, 398 (1966); J. Zucker, S. Zemon, and J. H. Wasko, in *International Conference on II-VI Semiconducting Compounds* 1967, edited by D. G. Thomas (Benjamin, New York, 1967), p. 919.

[19]V. L. Gurevich, Fiz. Tekh. Poluprov. 2, 1557 (1968) [Sov. Phys. Semicond. 2, 1299 (1969)].

[20]P. N. Butcher and N. R. Ogg, J. Phys. D 1, 1271 (1968); 2, 333 (1969); Phys. Letters 30A, 220 (1969); J. Phys. C 3, 706 (1970); P. N. Butcher, *ibid.* (to be published).

[21]B. K. Ridley and J. Wilkinson, J. Phys. C 2, 1299 (1969); 2, 1307 (1969); 2, 1321 (1969); B. K. Ridley, *ibid.* 3, 935 (1970).

[22]Yu. V. Gulyaev, IEEE Trans. Sonics Ultrasonics SU-17, 111 (1970); W. Wonnenburger, H. G. Reik, and A. Knoll, Phys. Letters 30A, 46 (1969); R. K. L. Gay and H. L. Hartnagel, J. Phys. D 2, 1589 (1969); 3, 736 (1970).

[23]S. Zemon, J. Zucker, J. H. Wasko, E. M. Conwell, and A. K. Ganguly, Appl. Phys. Letters 12, 378 (1968); S. Zemon, J. Zucker, and J. H. Wasko, Proc. IEEE 56, 778 (1968).

[24]M. Bruun, W. Wettling, and N. I. Meyer, Phys. Letters 31A, 31 (1970).

[25]D. S. Zoroglu and I. C. Chang, Phys. Letters 29A, 672 (1969).

[26]M. Schulz and B. K. Ridley, Phys. Letters 29A, 17 (1969); V. K. Komar and B. L. Timan, Fiz. Tverd. Tela 11, 3035 (1969) [Sov. Phys. Solid State 11, 2466 (1970)]; M. Schulz, Solid State Commun. 8, 355 (1970).

[27]G. D. Benedek and K. Fritsch, Phys. Rev. 149, 647 (1966).

[28]R. Bray and M. Simhony, Phys. Letters 29A, 540 (1969).

[29]D. L. Spears and R. Bray, Phys. Letters 29A, 542 (1969).

[30]G. Weinreich, Phys. Rev. 107, 317 (1957).

[31]K. R. Keller and B. Abeles, J. Appl. Phys. 37, 1937 (1966).

[32]B. A. Bobylev and A. F. Kravchenko, Akust. Zh. 12, 369 (1966) [Sov. Phys. Acoust. 12, 315 (1967)].

[33]D. L. Spears and R. Bray, Appl. Phys. Letters 13, 268 (1968); 14, 204 (E) (1969).

[34]P. K. Tien, Phys. Rev. 171, 970 (1968).

[35]C. Jacoboni and E. H. Prohofsky, Phys. Rev. B 1, 697 (1970).

[36]H. Ehrenreich, Phys. Rev. 120, 1949 (1960).

[37]For a review and other references, see M. Pomerantz, Proc. IEEE 53, 1438 (1965).

[38]A. Akhiezer, J. Phys. (USSR) 1, 277 (1939).

[39]W. P. Mason and T. B. Bateman, J. Acoust. Soc. Am. 36, 644 (1964); 40, 852 (1966).

[40]M. F. Lewis, J. Acoust. Soc. Am. 43, 852 (1968).

[41]P. B. Miller, Phys. Rev. 137A, 1937 (1965).

[42]M. G. Holland, IEEE Trans. Sonics Ultrasonics

SU-15, 18 (1968).
[43]L. E. Merkulov, Akust. Zh. 5, 439 (1959) [Sov. Phys. Acoust. 5, 444 (1960)].
[44]L. T. Claiborne, R. B. Hemphill, and N. G. Einspruch, J. Acoust. Soc. Am. 45, 1352 (1969).
[45]T. B. Bateman and J. H. McFee, J. Appl. Phys. 39, 4471 (1968).
[46]T. M. Fitzgerald, B. B. Chick, and R. Truell, J. Appl. Phys. 35, 2647 (1965).
[47]See, e.g., M. G. Holland, Phys. Rev. 134A. 471 (1964).
[48]C. M. Bhandari and G. S. Verma, Phys. Rev. 140A, 2101 (1965).
[49]R. Kishore, Phys. Rev. 173, 856 (1968).
[50]The fact that the lowest frequencies do not start their rapid decay immediately after voltage cutoff was somewhat puzzling. This slow start is evident at all flux levels. It may be the effect of lack of sufficient resolution in space and time. We found that for finer resolution the flux at the lowest frequency did indeed enter into its rapid decay more quickly.
[51]G. J. Robinson and M. B. N. Butler, Electron. Letters 5, 529 (1969).
[52]J. P. Rope, Phys. Status Solidi 21, 517 (1967).
[53]J. Zucker, S. A. Zemon, and J. H. Wasko, *Proceedings of the IXth International Conference on Physics of Semiconductors*, Vol. 2 (Nauka, Leningrad, 1968), p. 904.
[54]A. Ishida and Y. Inuishi, J. Phys. Soc. Japan 25, 640 (1968).
[55]In the calculation of the scattering cross section, another mechanism for scattering should be considered. It has been shown in the case of Raman scattering by optical phonons in piezoelectric crystals [see E. Burstein, S. Ushioda, and A. Pinczuk, Solid State Commun. 6, 407 (1968)] that the first-order time-dependent change in polarizability, electric susceptibility, and dielectric constant is determined by the relative atomic displacement coordinates and by the macroscopic electric field carried by the phonons. In analogy, the Brillouin-scattering cross section is determined by the change in dielectric constant $\delta\epsilon$, which depends on the strain S through the elasto-optic tensor p and, because the acoustic phonon carries a piezoelectric field E, also depends on E through the electro-optic tensor r. For small strains and electric fields, these dependences are given by $-\delta\epsilon_{ij}/\epsilon_\infty^2 = P_{ijkl}S_{kl} + r_{nij}E_n$. Considering the maximum value of $E = \epsilon S/\epsilon_\infty$ with the known values of $p_{44} = 0.072$ and $r_{41} = 1.2\times10^{-12}$ m/V at $\lambda_0 = 1\ \mu$ and the piezoelectric constant $e_{14} = 0.16$ C/m^2 pertinent for the fast TA phonons of interest, we estimate that the largest ratio of the electro-optic to the elasto-optic contribution to the change in dielectric constant is about 0.024, a negligible contribution in this particular case. Also, examination of the symmetry properties of r_{nij} and p_{ijkl} indicates that both contributions will produce the same polarization selection rule $A \perp P \parallel [001]$.
[56]A. Feldman and D. Horovitz, J. Appl. Phys. 39, 5598 (1968).

PHYSICAL REVIEW B VOLUME 3, NUMBER 10 15 MAY 1971

Relaxation-Time Ansatz for Quantum Transport Theory: Spin Effects*

R. W. Davies and F. A. Blum
Lincoln Laboratory, Massachusetts Institute of Technology, Lexington, Massachusetts 02173
(Received 11 December 1970)

A relaxation-time ansatz which treats both orbital and spin relaxation in quantum electron transport theory is presented. For orbital relaxation we use an ansatz which conserves both charge and spin density, and which is a modification of the treatment in which the collision processes are assumed to relax the system to a state of instantaneous local thermal equilibrium. For spin relaxation the ansatz conserves only the charge density. The general method yields gauge-invariant charge-conserving results for the response of the system to an electromagnetic perturbation, and yields physically correct results for the spin resonance response of the electronic system. General results are derived for the linear-response part of the one-electron density matrix for the case of a space- and time-varying perturbation corresponding to a single Fourier component. The results are applied to the calculation of the electrical conductivity, the magnetic susceptibility, and the cross section for inelastic light scattering from semiconductor magnetoplasmas.

I. INTRODUCTION

In many calculations of quantum transport processes, a useful first approximation is to treat the effect of collisions on the carriers by introducing a phenomenological relaxation-time term into the transport equation. If the relaxation time τ is measured in one experiment, and if it does not vary rapidly with frequency, then the value obtained can be applied to analyze other experimental situations. Though simple in essence, the use of a relaxation-time ansatz in quantum transport theory is not without its hazards. Naive forms of the ansatz fail (a) to conserve charge and/or (b) to give gauge-invariant results. This latter difficulty is circumvented in classical or semiclassical treatments because the transport equation is formulated directly in terms of the electromagnetic fields

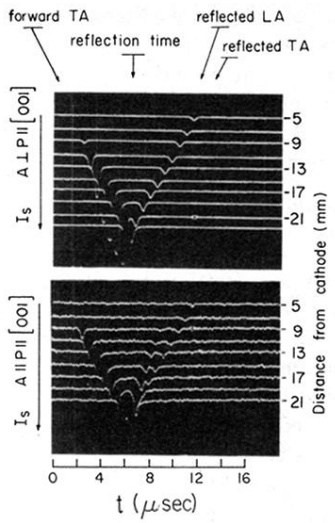

FIG. 2. Top oscilloscope traces in (a) show scattering signals for the forward-propagating and reflected TA phonon domain for the crossed polarizer and analyzer combination required to observe single scattering. Bottom oscilloscope traces in (b) show the forward-propagating TA domain and both the reflected TA and LA domains. Here, a parallel polarizer and analyzer combination is used as required to see the LA domain. Nevertheless, the weak TA domain signals appear in (b) by virtue of double Brillouin scattering in the intense phonon flux, which permits the violation of the crossed-polarization requirement discussed in the text. For $\theta = 7°$ and $\psi = 4°$ we see here 0.41-GHz TA phonons in the single-scattering case and 0.64-GHz LA phonons traveling $\sim 1°$ off axis.

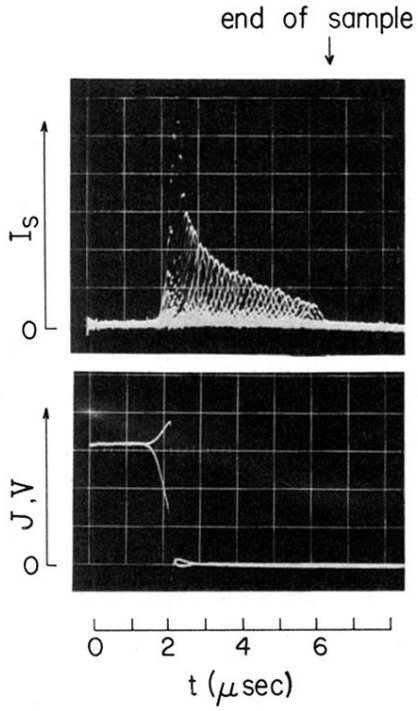

FIG. 3. Envelope of scattering signals I_s as a function of time for the light spot moved progressively down the sample; $\theta = 18°$, $f = 1.04$ GHz, and $A \perp P \parallel [001]$. From the accompanying current and voltage pulses, we see that the domain signal switches from growth to attenuation when the voltage is cut off.

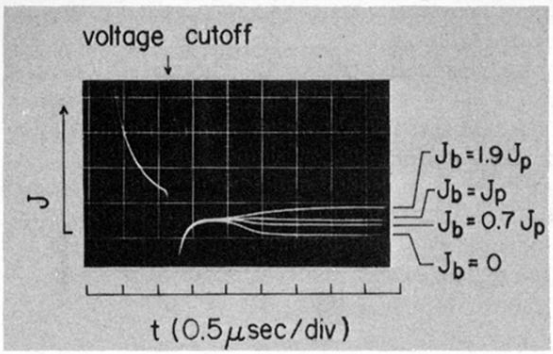

FIG. 6. Current traces for various biasing voltages, represented here by the corresponding ultimate bias currents J_b. The bias voltage in the form of a long low voltage pulse is applied shortly after cutoff of the primary voltage. A common plateau in the current persists for all bias voltages until the flux decays sufficiently to allow the sample to return to its Ohmic condition. The currents then approach their Ohmic bias levels at different rates.